

# Analytical Methods

Accepted Manuscript



This is an *Accepted Manuscript*, which has been through the Royal Society of Chemistry peer review process and has been accepted for publication.

*Accepted Manuscripts* are published online shortly after acceptance, before technical editing, formatting and proof reading. Using this free service, authors can make their results available to the community, in citable form, before we publish the edited article. We will replace this *Accepted Manuscript* with the edited and formatted *Advance Article* as soon as it is available.

You can find more information about *Accepted Manuscripts* in the [Information for Authors](#).

Please note that technical editing may introduce minor changes to the text and/or graphics, which may alter content. The journal's standard [Terms & Conditions](#) and the [Ethical guidelines](#) still apply. In no event shall the Royal Society of Chemistry be held responsible for any errors or omissions in this *Accepted Manuscript* or any consequences arising from the use of any information it contains.

## ARTICLE

# Quantification of Arsenic (III) in Aqueous Media using a Novel Hybrid Platform Comprised of Radially Porous Silica Particles and a Gold Thin Film

Y. Choi<sup>a1</sup>, H. Kwak<sup>b1</sup> and S. Hong<sup>b\*</sup>

Received 10th January 2012,

Accepted 10th January 2012

DOI: 10.1039/c2ay20000x

www.rsc.org/

The use of novel radially porous silica particles and gold thin film hybrid-based spectroscopy for the sensitive and anion-selective detection of As(III) is described. The method is based on the selective formation of electrostatic complexes between As(III) and an amine functionality on the porous silica particles and the effect of this on changes in the surface plasmon resonance (SPR) profiles of the gold thin film. Since silica particles have radially oriented mesopores, the sizes of which gradually increase from the center to outer surface of the particle, they provide very large surface area, and permit target analytes to easily access active receptors within the pores. Thus, the amine-functionalized silica particles contain a much higher concentration As(III) receptors than conventional porous nanoparticles or a flat surface, which results in a lower detection limit. In addition, due to the surface property of silica as a dielectric spacing layer, it allows the sensing platform to be more sensitive and stable. The SPR properties of the resulting selectively formed complexes are altered, leading to significant changes in SPR reflectance ( $\Delta R$ ) near the SPR angle. The limit of detection of the method was determined to be 1.0 nM, which is *ca.* 80 times more sensitive than the U.S. EPA regulation level (10  $\mu\text{g/L} \approx 130$  nM). The response is essentially linear in the concentration range of 10 ~ 600 nM on a semi-log scale. The method also shows good selectivity for As(III) in the presence of  $\text{H}_2\text{PO}_4^-$ ,  $\text{SO}_4^{2-}$ ,  $\text{NO}_3^-$ , and  $\text{Cl}^-$  and is feasible for use in the analysis of tap (drinking) water; therefore, it would be applicable for use in environmental and biological monitoring.

## Introduction

The threat of arsenic pollution in aqueous media is a serious environmental and health concern because of its toxic and carcinogenic effects on humans and other living organisms. The total-arsenic level in drinking water should be below 10 ppb as regulated by the World Health Organization (WHO).<sup>1</sup> The main species of arsenic found in the environment are arsenic(III) and arsenic(V) oxyacids. In many environments, arsenic(V) is frequently deprotonated and is present in the form of an anion, and arsenate ( $\text{AsO}_4^{3-}$ ), hydrogen arsenate ( $\text{HAsO}_4^{2-}$ ), and dihydrogen arsenate ( $\text{H}_2\text{AsO}_4^-$ ) ions, which constitute the most common forms of arsenic in contaminated soil and groundwater.<sup>2</sup> Therefore the development of analytical methods for quantifying trace levels of arsenic has become an urgent objective.

A wide variety of analytical techniques and methods for the determination of arsenic have been developed. Spectroscopic techniques, including atomic absorption spectroscopy,<sup>3</sup> hydride generation atomic absorption spectroscopy,<sup>4</sup> inductively coupled plasma-mass spectroscopy,<sup>5</sup> atomic fluorescence spectroscopy,<sup>6</sup> and chromatographic techniques such as liquid chromatography<sup>7</sup> and ion chromatography<sup>8</sup> are in widespread use for the detection of arsenic compounds. However, these conventional established techniques have significant limitations, which include spectral and chemical interference and the need for complicated instrumentation. They also involve sample preservation and chemical reduction steps,

which can serve as a source of sample contamination and can also prolong turnout time. Thus, it is difficult to apply such analyses in the field and in real time monitoring, and *in situ* measurements are highly desirable because they permit the early detection of problems while minimizing errors, labor and cost associated with the spectroscopic methods.

A number of alternative methods involving the use of chemical and biosensors, i.e., electrical<sup>9</sup> and electrochemical methods,<sup>10</sup> and optical methods including fluorescent biosensors,<sup>11</sup> surface plasmon resonance measurements,<sup>12</sup> laser induced breakdown spectroscopy,<sup>13</sup> and colorimetric assays<sup>14</sup> have been proposed. Among them, surface plasmon resonance (SPR)-based optical detection methods have been of interest in terms of sensitivity and *in situ* real-time monitoring, which involves the use of molecules/receptor interactions at a noble metal layer based on the change in refractive index at the interface.<sup>15</sup> While the SPR technique has certain advantages and because the sensitivity of the method is sufficient for monitoring target analytes, further efforts directed toward signal enhancement are still required and the determination of trace amounts of analytes continues to be a challenging task.

In addition, to date, cationic metal ion-selective detection methods have been shown to be successful and are frequently used in clinical and environmental analyses. However, the design of an arsenic-selective sensor and controlling its selectivity in the presence of various anions has proven to be difficult due to the wide range of co-contaminating species, low-charge to radii ratios, sensitivity to pH and high solvation

energies of these species;<sup>16</sup> methods for the direct analysis and an anion-selective sensor for arsenic are not currently readily available. In this regards, the development of an anion-selective quantification method for arsenic would be highly desirable.

Here, we report on a highly sensitive and anion-selective method for the detection of As(III), based on a signal-enhanced SPR sensor using a novel hybrid platform comprised of radially porous silica particles and a gold thin film. The method involves the selective formation of a complex between As(III) and an amine ligand via electrostatic interactions and the signal-enhanced plasmon modes of the hybrid complexes. The method has several advantages over existing methods. Since the silica particles have radially oriented mesopores, in which their size gradually increases in proceeding from the center to the outer surface of the particle, they provide very large surface area, and permit target analytes to easily access the active receptors that are located within the pores. Thus, amine-functionalized silica particles are capable of containing a much higher concentration of As(III) receptors than conventional porous nanoparticles or a flat surface, resulting in a lower detection limit. In addition, due to the surface property of silica as a dielectric spacing layer,<sup>17</sup> it allows the sensing platform to be more sensitive and stable. Furthermore, because As(III)-selective complexation of the ligand and an *in situ* detection system are involved, a high selectivity for other relevant anions, such as  $\text{H}_2\text{PO}_4^-$ ,  $\text{SO}_4^{2-}$ ,  $\text{NO}_3^-$ , and  $\text{Cl}^-$  and its feasibility for use in the analysis of drinking water is potentially possible. In this sense, this approach represents a promising method for determining As(III). Finally, the combination of these advantages results in a more sensitive, selective and reliable method for the determination of As(III). Because of this, the SPR hybrid platform-based detection method has considerable potential for use in environmental and biological applications.

## Experimental

### Materials

3-Mercaptoundecanoic acid (MUA, Sigma-aldrich Korea Ltd.), N-(3-dimethylaminopropyl)-N-ethylcarbodiimide (EDC, Sigma-aldrich Korea Ltd.), N-hydroxysuccinimide (NHS, Sigma-aldrich Korea Ltd.), hydrogen peroxide ( $\text{H}_2\text{O}_2$ , Sigma-aldrich Korea Ltd.), sulfuric acid ( $\text{H}_2\text{SO}_4$ , Fisher Scientific Korea Ltd.) were used to modify gold chip (gold thin film on glass substrates, K-MAC Korea Ltd.) surfaces. A piranha solution (70 %  $\text{H}_2\text{SO}_4$  and 30 %  $\text{H}_2\text{O}_2$ ) was used to clean the gold chips. Tetraethyl orthosilicate (99 %, Sigma-aldrich Korea Ltd.) was used as silica precursors. Cetylpyridinium bromide hydrate (98 %, Sigma-aldrich Korea Ltd.), cyclohexane (99 %, Sigma-aldrich Korea Ltd.) and 1-pentanol (99 %, Samchun Korea Ltd.) were utilized as the surfactant, organic phase and co-solvent, respectively, in the microemulsions. Urea and HCl, 3-Aminopropyltrimethoxysilane (97 %) and anhydrous toluene were purchased from Sigma-aldrich. Sodium arsenate dibasic heptahydrate ( $\text{Na}_2\text{HAsO}_4 \cdot 7\text{H}_2\text{O}$ ), sodium sulfate anhydrous ( $\text{Na}_2\text{SO}_4$ ), sodium phosphate dibasic ( $\text{Na}_2\text{HPO}_4$ ), sodium chloride (NaCl), sodium nitrate ( $\text{NaNO}_3$ ) were purchased from Sigma Korea and were used to determine sensing performance. All chemicals were used as received.

### Fabrication of radially porous silica particles and amine functionalization

Radially porous silica particles were prepared by modifying the microemulsion method.<sup>18</sup> In a typical synthesis, an aqueous

solution was prepared by dissolving 1 g of cetylpyridinium bromide hydrate and 0.6 g of urea in 30 mL of distilled water. In addition, an organic solution was prepared by mixing 2.5 g of tetraethyl orthosilicate, 30 mL of cyclohexane and 1.5 mL of 1-pentanol. The aqueous solution was mixed with the organic solution, and then stirred for 30 min at room temperature. The mixed solution was loaded into a glass-lined autoclave and hydrothermally treated under autogeneous pressure at 120 °C for 4 h. After hydrothermal treatment, as-prepared silica particles were collected by centrifugation, and then washed with a solution of acetone and water. The washed silica particles were dried at room temperature for 24 h, and then calcined in air at 550 °C for 6 h. Amine-functionalization was carried out by using the post-grafting method.<sup>19</sup> 2 g of radially porous silica particles was mixed with 50 mL of anhydrous toluene and 7 mL of 3-Aminopropyltrimethoxysilane. The mixture was refluxed for 48 h, and then filtered. The obtained solid was washed with acetone and chloroform, followed by drying for 12 h at 60 °C.

### Characterization of the silica particles

Scanning electron microscopy (SEM) images were obtained on a Carl Zeiss SUPRA 55VP field-emission scanning electron microscope. Transmission electron microscopy (TEM) observations were carried out on a JEOL JEM-3010 microscope operating at 300kV. The elemental compositions of solid products were investigated by an electron probe microanalysis (EPMA) using a JEOL JXA-8900R spectrometer.  $\text{N}_2$  adsorption-desorption isotherms were measured at -196 °C using a Micrometrics ASAP-2010 system. Pore size distribution curves were obtained from the adsorption branches of the isotherms using the Barrett-Joyner-Halenda (BJH) method.

### Modification of hybrid platform with porous silica particles and gold thin film

The gold thin film modified with MUA was prepared to immobilize the amine-functionalized porous silica particles on the substrates. A two-step procedure was used in preparing the functionalized and activated gold thin film. In the first step, a self-assembled monolayer (SAM) of MUA on the gold thin film was prepared by treating it overnight with a 1.0 mM ethanolic MUA solution. In the second step, the COOH groups of MUA were converted to reactive esters by reaction with NHS and EDC,<sup>20</sup> followed by a reaction to tether the amine-functionalized silica particles to the surface of the gold thin film. The surface of the functional group was protonated by a treatment with HCl (pH  $\approx$  2) for 3 min.

### SPR measurements

A flow cell (50  $\mu\text{L}/\text{min}$ ) was mounted on the sensor/prism assembly so that solution of interest could be introduced easily to flow across the Au surface and that switching between different solutions could be accomplished rapidly (SPR *micro*, K-mac Korea Ltd.). The SPR system was utilized in the Kretschmann configuration using attenuated total reflection (ATR). Time-resolved SPR angle shifts were measured using the fixed angle method which enabled the reflectance change  $\Delta R$  to be linearly correlated with the SPR angle shift,  $\Delta\theta_{\text{SPR}}$ . Reflectance data at a fixed incident angle were acquired in real time on a computer.<sup>21</sup>



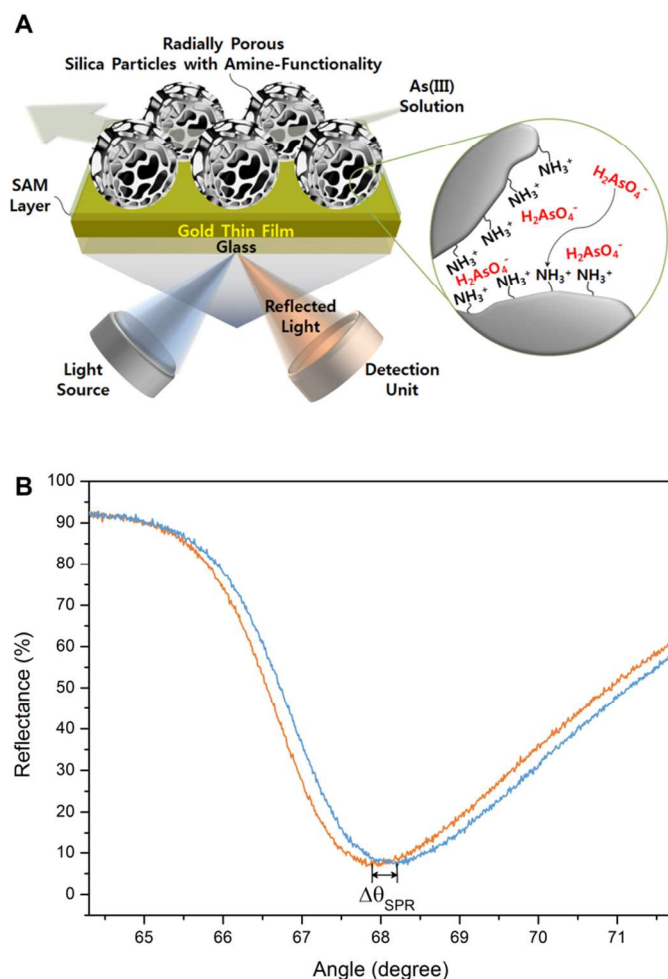


**Fig. 1** (A) Schematic diagram for the detection of As(III) using a hybrid platform of radially porous silica particles and a gold thin film via SPR spectroscopy. The enlarged schematic diagram shows the structure of the ligand on pores of the silica particles and the binding of As(III). (B) The corresponding SPR spectra before (orange line) and after (blue line) 1 h-exposure to 400 nM of As(III).

### Detection of As(III)

A standard solution of As(III) was prepared by dissolving  $\text{Na}_2\text{HAsO}_4$  in DI water. The pH of the solution was adjusted ( $\text{pH} \approx 6.7$ ) for the stable detection of As(III). The As(III) solutions in a concentration range from 1.0 nM (*ca.* 0.13 ppb) to 1.0  $\mu\text{M}$  were injected into an inlet of the sample well on the modified gold thin film, and real-time signals under flow conditions were measured. The surface plasmon signals of the interface of the gold thin film induced by the interaction between ligands and As(III) were then measured. Signal changes in reflectance were collected and the standard deviation for each concentration of As(III) was determined. The selectivity test toward  $\text{H}_2\text{PO}_4^-$ ,  $\text{SO}_4^{2-}$ ,  $\text{NO}_3^-$ , and  $\text{Cl}^-$  was performed using the same procedure as was used for the determination of As(III).

## Results and discussion

### Principles of amine-functionalized silica particles and gold thin film hybrid-based sensing

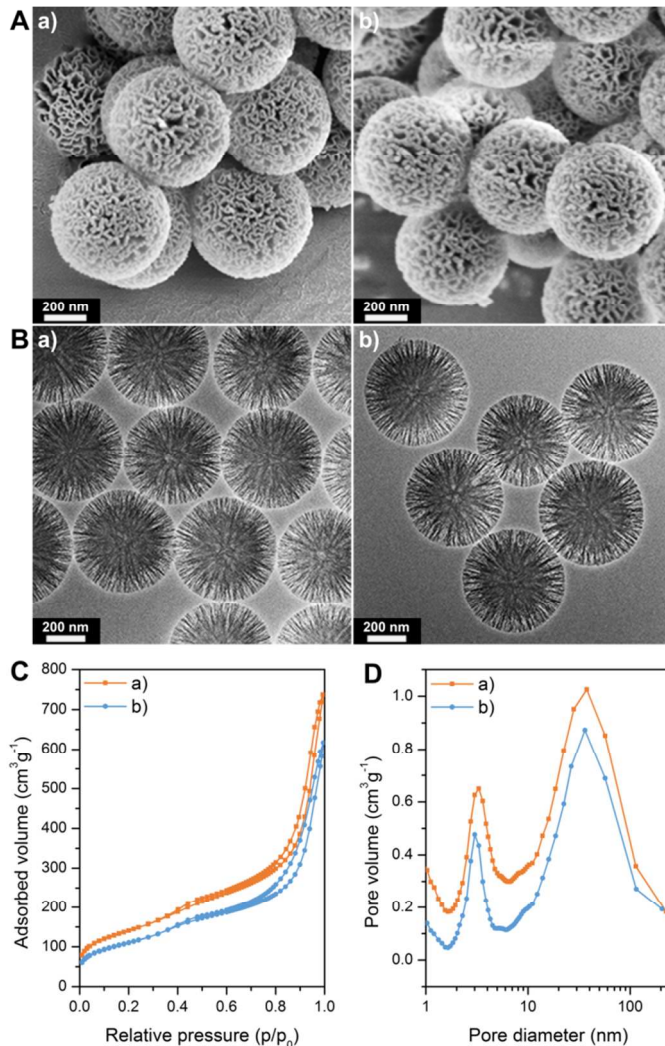


**Fig. 2** (A) SEM images, and (B) TEM images of the synthesized radially porous silica particles before (a) and after amine functionalization (b). The scale bar in the image is 200 nm. (C)  $\text{N}_2$  adsorption-desorption isotherm for the silica particles, and (D) BJH adsorption pore size distribution curves of the silica particles before (a) and after amine functionalization (b).

The SPR hybrid platform-based detection method involves the use of amine-functionalized radially porous silica particles, which function as a selective ligand for As(III), a gold thin film with the silica particles as a signal amplifier and a stabilizer of the surface chemistry in the sensing platform, and SPR measurements for the detection of the interface of the sensor substrate. The overall scheme for the analytical method is shown in Fig. 1A. It has been reported that dihydrogen arsenate has an affinity for amine groups via hydrogen-bond formation<sup>22</sup> and that arsenic has a tendency to form two-coordinated metal complexes with amine groups.<sup>23</sup> To induce the electrostatic interaction and enhance the affinity for binding of As(III) to the amine ligand, the terminal group of the functionalized silica particles was altered from  $-\text{NH}_2$  to  $-\text{NH}_3^+$  by a treatment under acidic condition. Despite the fact that a  $\text{HAsO}_4^{2-}/\text{H}_2\text{AsO}_4^-$  mixture ( $\text{p}K_a \approx 6.76$ ) is dominant under typical conditions, only  $\text{H}_2\text{AsO}_4^-$  is shown in the schematic representation.

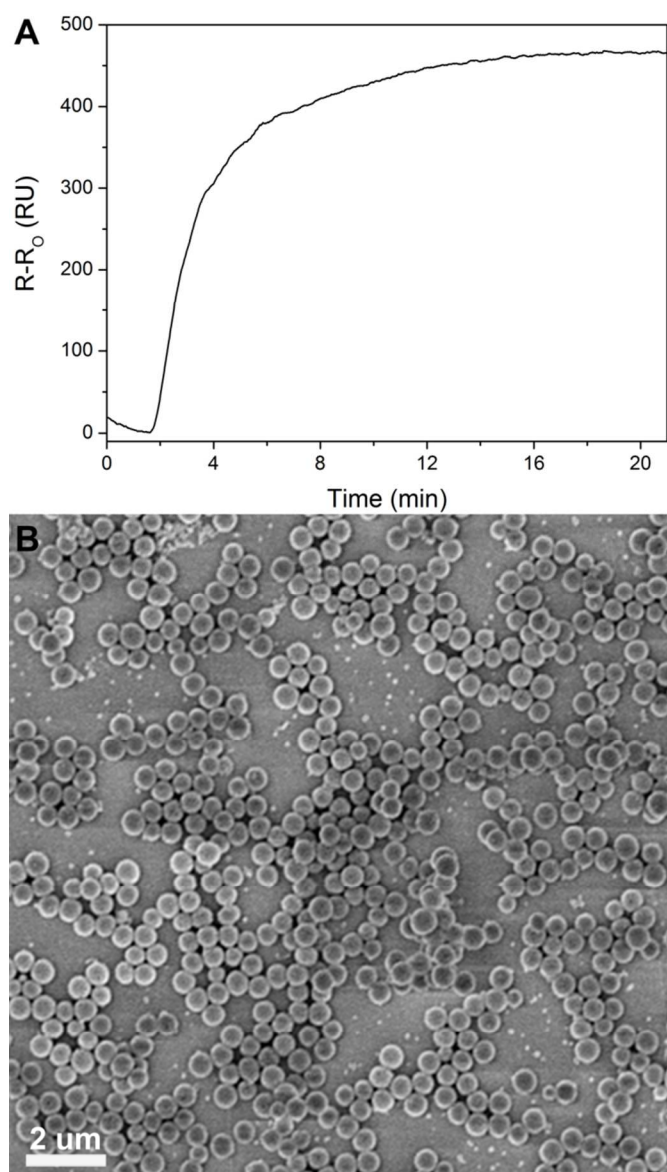


**Fig. 3** (A) Time-resolved SPR signal for the immobilization of radially porous silica particles onto the gold thin film. (B) SEM image of the immobilized silica particles on the gold thin film. The scale bar in the image is 2.0  $\mu\text{m}$ .

Since the silica particles have radially oriented mesopores and their size gradually increases from the center to the outer surface of the particle, they provide very large surface area, and permit target analytes to easily access the active receptors within the pores. The amine-functionalized silica particles, therefore, provide a much higher concentration of arsenic receptors than conventional porous nanoparticles or a flat surface, which results in a lower detection limit. In addition, because the surface property of silica particles function as a dielectric spacing layer, which can function as spatially extended probes of interfacial electric fields for amplified signal transduction in the SPR system, it permits the sensing platform to be more sensitive and stable. Therefore, the integration of widely distributed binding sites and the dielectric property of the interfacial sensing layer as a signal amplifier can induce significant changes in the optical constants.

Upon the binding of As(III) to the sensor surface, the As(III) undergoes selective complexation with the ligand of amine on the radially mesoporous silica particles-gold thin film hybrid via electrostatic interactions, resulting in significant changes in the SPR curve profiles. Fig. 1B shows a representative SPR contour plot for the sensing at an As(III) concentration of 400 nM. The SPR plot shows a measurable spectral shift ( $\Delta\theta_{\text{SPR}} \approx 0.4^\circ$ ), which can be explained by a change in the local refractive index adjacent to the interface of the sensor surface.

#### Characteristics of silica particles and gold thin film hybrids

Electron microscopic analyses were used to investigate the morphology and structure of the radially porous silica particles. In the SEM image shown in Fig. 2A, prior to amine-functionalization, the silica particles have a uniform spherical shape with an average diameter of 500 ~ 600 nm. A close inspection of the SEM image reveals that the silica particles are composed of many wrinkled sheets. These wrinkled sheets are arranged in three dimensions to form the spherical particles, and the void space between the sheets form silt-shaped pores with a large pore mouth of 15 ~ 50 nm. The TEM image of Fig. 2B clearly confirms that the pores of the silica particles are radially oriented, and that the pore size gradually increases from the center to the outer surface of the particles.

It should be noted that, even after the amine functionalization, the unique pore structures of the silica particles remained well maintained as shown in Fig. 2C. This result implies that the amine-functional groups are well distributed on the internal surface of the pores in the silica particles without inducing the collapse of the pore structures. These radially porous structures with large pore openings are capable of facilitating the easy diffusion of target analytes into the internal surface, leading to the rapid detection of As(III).

The pore structures of the silica particles, before and after amine functionalization, were further investigated by  $\text{N}_2$  adsorption-desorption measurements. Both types of silica particles had a very similar isotherm. All showed a type IV isotherm with a  $\text{H}_3$  type hysteresis loop in the  $P/P_0$  range of 0.4 ~ 1.0, indicating the presence of various sized, slit-shaped mesopores.<sup>24</sup> The only difference was that the BET surface area was slightly decreased from 504 to 457  $\text{m}^2/\text{g}$  after the amine-functionalization. The BJH adsorption pore volume curves (Fig. 2D) clearly reveal that the amine functionalization causes a slight shrinkage and/or blockage of small sized pores, resulting in a decrease in overall surface area.

The amine-functionalized silica particles were then immobilized on gold thin films via carboimide coupling to amine moieties of the silica particles to prepare the SPR sensor surfaces for the determination of As(III). The kinetics of binding of the silica particles on the gold thin film was measured by time-resolved SPR measurements (Fig. 3A). The results suggest that the immobilization of the silica particles on the gold thin film was complete within 10 min due to the strong affinity between the 2 reactants. Fig. 3B shows an SEM image of the surface of a gold thin film on which the amine-functionalized silica particles are immobilized. The distribution of the silica particle is uniform and resembles a monolayer. Although there are some vacant particles on the gold thin film, it can be concluded that the effect of this on sensing performance is negligible, because the SPR signals are obtained by averaging the values across a light source-scanning area of ca. 1.0  $\text{mm}^2$ .



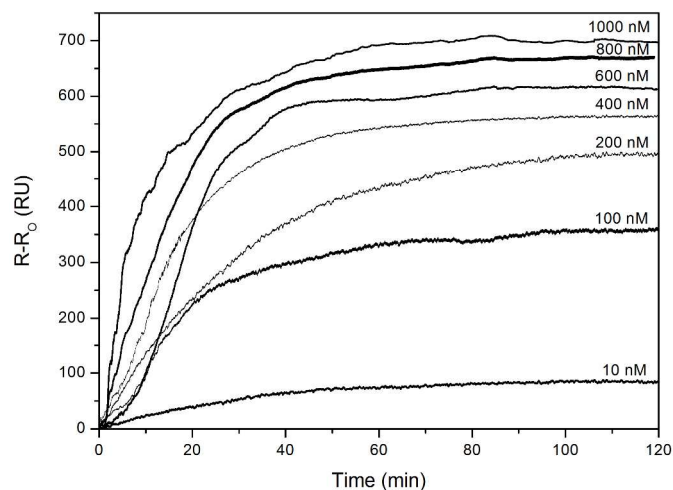


**Fig. 4** Time-resolved changes in the SPR signal (Reflectance,  $\Delta R$ ) in the fixed angle mode for the in situ monitoring of As(III) concentrations in the range of 10 nM to 1.0  $\mu\text{M}$ .

#### Response time of the silica particles and gold thin film hybrids in As(III) solution

With the basic principles in hand, the real-time sensing performance of the sensor surface was first investigated to examine the dependence of the surface sensitivity originating from the interaction between the sensing layer of the silica particles and As(III). In order to analyze the real time response of the sensor surface, the radially porous silica particles-modified gold thin film was directly exposed to As(III) solutions. The changes in reflectance near the SPR angle were measured and the time-resolved SPR signal change in reflectance was obtained by the fixed-angle mode.

Interestingly, an exposure time of only about 30 min was needed for the discrimination of As(III) concentrations in the measured range. Based on the shape of the graph and the change in SPR signal of each As(III) concentration, it would be possible to estimate the concentration of As(III) within a period of 30 min. It is also noteworthy that the concentration of the injected sample would be higher than the EPA regulation level (10  $\mu\text{g/L} \approx 130$  nM) if the SPR signals were to increase to over *ca.* 300 R.U. for a 30 min detection time. When an SPR signal lower than 300 RU is observed within the detection time, the sample concentration would be lower than the EPA regulation level. As a result, the concentration of As(III) in an actual sample of contaminated water can be sensitively monitored in real time, within 30 min using SPR signals as the criterion. The rapid response time can be partly attributed to the unique radially porous structure of the silica particles and the electrostatic complexation of As(III) with the amine functionality on the silica particles as well.

#### Exploration of sensitivity and determination of As(III)

To examine the sensitivity of the method and determine As(III) concentrations in real waste samples, the optimized detection time for the method was first evaluated for various As(III) concentrations, since this issue would be of practical interest in the analysis of As(III). An insufficient detection time results in a low coverage of As(III) on the surface and leads to a lower sensitivity, whereas an overly long detection time may result in the formation of multiple layers of As(III), leading to the blockage of binding sites and a lower efficiency. Based on the results shown in Fig. 4, we confirmed that the optimized detection time would be 1 h, which is a sufficient time for the

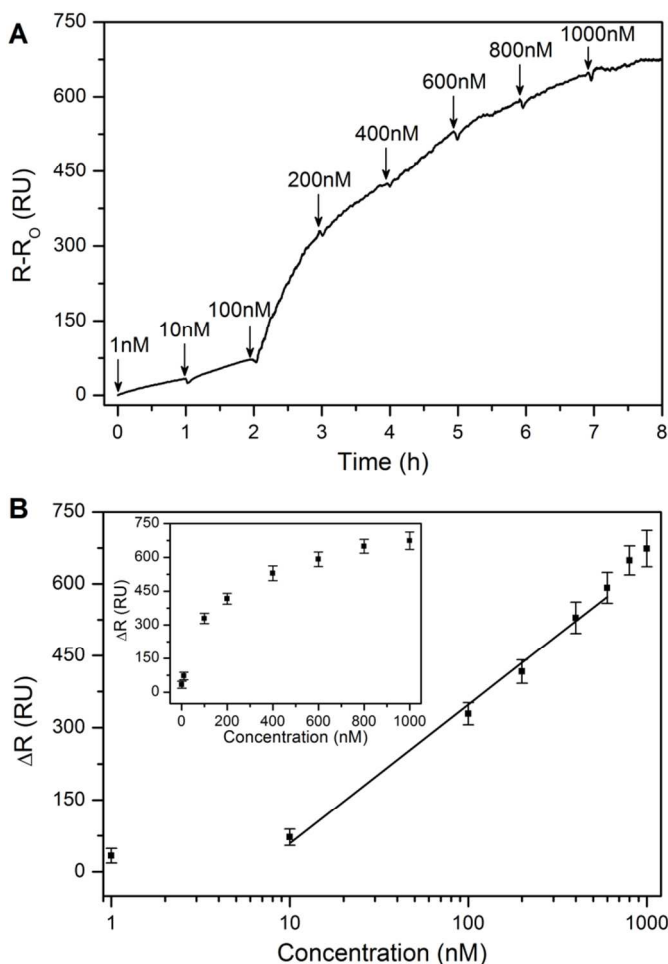


**Fig. 5** (A) Time-resolved change in reflectance ( $\Delta R$ ) near the SPR angle following the angle shifts measured for successive different concentrations of As(III) in the range of 1.0 nM to 1.0  $\mu\text{M}$ . (B) The calibration curve for As(III) as a function of concentrations from 1.0 nM to 1.0  $\mu\text{M}$  on a semi-log scale. The error bar shown is the standard deviation from the mean ( $n=3$ ). The inner graph is the SPR signal changes as a function of As(III) concentrations without log scale.

various As(III) concentrations used to reach equilibrium. Thus, in order to explore the sensitivity of the method, the changes in the SPR reflectance after a 1 h-exposure were determined for As(III) concentrations in the range of 1.0 nM to 1.0  $\mu\text{M}$ .

When the sensor surface is exposed to an As(III) solution, the SPR angle position is right-shifted, compared to the silica particles modified with a gold thin film before the detection. The SPR angle shifts proportionally to a larger SPR angle with increasing concentrations of As(III). The subsequent change in reflectance ( $\Delta R$ ) near the SPR angle following the angle shifts measured for different concentrations is shown in Fig. 5A. As the concentration of As(III) is increased, the SPR reflectance signal increases. To construct a calibration curve, the sensor response was read after 1 h and determined as a function of analyte concentration. Fig. 5B shows the calibration curves for the method for As(III). The results were created using SPR responses for a minimum of 3 substrates. Concerning signal noise (the SPR reflectance of the thin film fluctuated within *ca.*  $\pm 3.0$  RU in aqueous media in the absence of As(III).), the limit of detection (LOD) was determined to be less than 1.0 nM, which makes the method approximately 80 times more

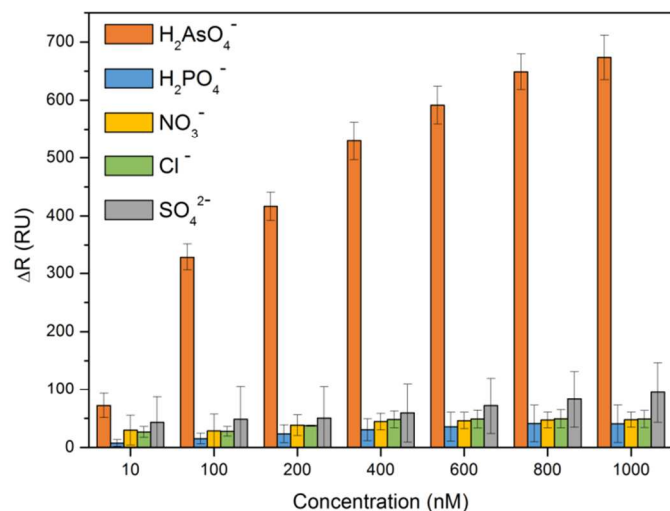


**Fig. 6** SPR signal changes in  $\Delta R$  of a sensor surface after exposure to concentrations of 10 nM to 1.0  $\mu\text{M}$  of  $\text{H}_2\text{AsO}_4^-$ ,  $\text{H}_2\text{PO}_4^-$ ,  $\text{SO}_4^{2-}$ ,  $\text{NO}_3^-$ , and  $\text{Cl}^-$ , respectively. The error bar shown is the standard derivation from the mean ( $n=3$ ).

sensitive than the current EPA regulation level (10  $\mu\text{g/L} \approx 130$  nM) for As(III) in drinking water. The high sensitivity of the method results from the large distribution of binding sites for As(III) and the spatially extended probe of interfacial electric fields on the hybrid platform comprised of radially porous silica and a gold thin film.

It should be noted that the response of the SPR signals for As(III) are quite linear in the range of 10 ~ 600 nM on a semi-log scale. At higher concentrations of As(III), the formation of electrostatic complexes became saturated, leading to a nonlinear response and a plateau, for concentrations above 800 nM. The reason for the nonlinear response at higher As(III) concentrations is that the amine ligand on the silica particles becomes nearly saturated with As(III) ions and, as a result, complex formation between the ligand and As(III) decreases drastically. That is, the change in SPR reflectance initially is increased in the population to the As(III) concentration, and ultimately reaches a limiting value ( $\Delta R \approx 670$  RU).

#### Evaluation of selectivity of As(III)

We also tested the selectivity of the method for As(III) in the presence of other environmentally relevant anions, including  $\text{H}_2\text{PO}_4^-$ ,  $\text{SO}_4^{2-}$ ,  $\text{NO}_3^-$ , and  $\text{Cl}^-$ . The response of the SPR profiles to aqueous solutions of the above analytes in the range of 10 nM ~ 1.0  $\mu\text{M}$  is shown in Fig. 6. The results show that a more than 10 times excess of various potential interfering ions had no obvious influence on the determination of As(III). The method showed a high specificity and reliability for a As(III) assay. It is noteworthy that, although the selective detection of As(III) in the presence of phosphate is known to be difficult due to the fact that the two ions are similar; the change in the SPR response for As(III) was clearly different from that for phosphate.

#### Feasibility test in drinking water

In order to evaluate the feasibility of the method for actual water sample analysis, we further used the method to measure As(III) in actual samples of drinking tap water. Tap water samples were collected from our laboratory after allowing the water to flow for about 3 min. The water samples were directly analyzed and were found to be free of arsenic contamination

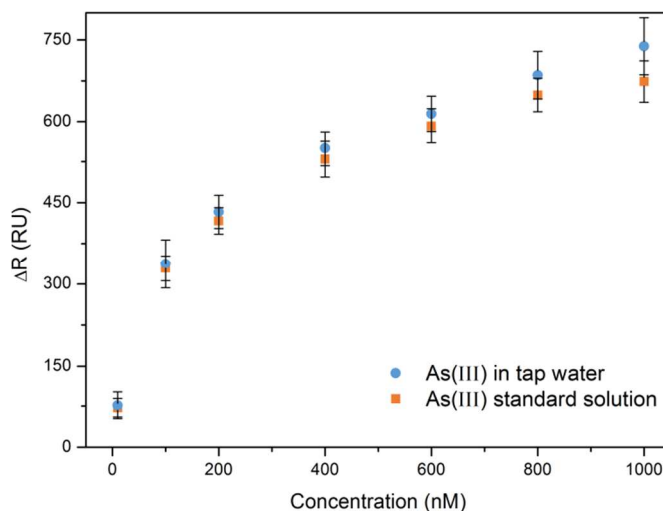


**Fig. 7** Quantitative correlations for As(III) determination in tap water samples as a function of concentrations of 1.0 nM to 1.0  $\mu\text{M}$ . The error bar shown is the standard derivation from the mean ( $n=3$ ).

before the spiking procedure. Quantitation correlations assessed using samples spiked at different concentration levels were obtained between change in reflectance ( $\Delta R$ ) near the SPR angle and corresponding concentrations of As(III) as shown in Fig. 7. The results suggest that the developed SPR hybrid platform-based detection method has the potential for use in the analysis of real samples without significant matrix interference. Therefore, the method would be applicable to the analysis of As(III) in environmental and drinking water samples.

#### Conclusions

In conclusion, an SPR sensing platform for the sensitive, anion-selective detection and quantification of As(III) using radially porous silica particles and gold thin film hybrid is described. The basis for the sensing method involves the electrostatic and selective complexation of As(III) with amine groups by a radially mesoporous silica particles-modified gold thin film, which results in significant changes in the SPR profiles. The limit of detection was determined to be 1.0 nM, which is *ca.* 80 times more sensitive than the U.S. EPA regulation levels. A linear response was observed for As(III) concentrations in the range of 10 nM ~ 600 nM in a semi-log scale. The sensing response is highly selective for As(III) over other anions, including  $\text{H}_2\text{PO}_4^-$ ,  $\text{SO}_4^{2-}$ ,  $\text{NO}_3^-$ , and  $\text{Cl}^-$ . Furthermore, the sensing platform was also feasible for use in the analysis of tap water (drinking water). We conclude that the proposed analytical method can be applied to other areas, such as biosensing and environmental monitoring as well.

#### Acknowledgements

This work was supported by Basic Science Research Program through the National Research Foundation of Korea (NRF) funded by the Ministry of Science, ICT & Future Planning (2013-0067).

#### Notes and references

<sup>a</sup> Institute of Technology, SK Innovation Global Technology, Daejeon 305-712, Korea.

- <sup>b</sup> Department of Applied Bioscience, CHA University, Gyeonggi-do 463-863, Korea. \*E-mail: [hongsr@cha.ac.kr](mailto:hongsr@cha.ac.kr); Fax: +82 31 725 8350; Tel: +82 31 725 8262
- <sup>1</sup> equally contributed authors (co-first author)
- 1 Y. Kim, C. Kim, I. Choi, S. Rengaraji and J. Yi, *Environ. Sci. Technol.*, 2004, **38**, 924; Y. He, Y. Zheng, M. Ramnaraine and D.C. Locke, *Anal. Chim. Acta*, 2004, **51**, 55.
  - 2 S. Hong, S. Park, S. Lee, Y. I. Yang, H. D. Song and J. Yi, *Anal. Chim. Acta*, 2011, **694**, 136; D. Melamed, *Anal. Chim. Acta*, 2005, **532**, 1.
  - 3 R. H. Atallah and D. A. Kalman, *Talanta*, 1991, **38**, 167.
  - 4 H. Md Anawar, *Talanta*, 2012, **88**, 30; A. N. Anthemidis and E. K. Martavaltzoglou, *Anal. Chim. Acta*, 2006, **573**, 413.
  - 5 S. Mazan, G. Crétier, N. Gilon, J. -M. Mermet and J. -L. Rocca, *Anal. Chem.*, 2002, **74**, 1281; P. G. Smith, L. Koch and K. J. Reimer, *Environ. Sci. Technol.*, 2007, **41**, 6947.
  - 6 X. -P. Yan, X. -B. Yin, X. -W. He and Y. Jiang, *Anal. Chem.*, 2002, **74**, 2162.
  - 7 C. B'Hymer and J. A. Caruso, *J. Chromatogr. A*, 2004, **1045**, 1.
  - 8 D. T. Heitkemper, N. P. Vela, K. R. Stewart and C. S. Westphal, *J. Anal. At. Spectrom.*, 2001, **16**, 299.
  - 9 Y. Liu, Z. Huang, Q. Xie, L. Sun, T. Gu, L. Bu, S. Yao, X. Tu, X. Luo and S. Luo, *Sens. Act. B*, 2013, **188**, 894; S. Prakash, T. Chakrabarty, A. K. Singh and V. K. Shahi, *Electrochim. Acta*, 2012, **72**, 157; D. E. Mays and A. Hussam, *Anal. Chim. Acta*, 2009, **646**, 6.
  - 10 J. -F. Huang and H. -H. Chen, *Talanta*, 2013, **116**, 852; L. Chen, N. Zhou, J. Li, Z. Chen, C. Liao and J. Chen, *Analyst*, 2011, **136**, 4526; Y. Du, W. Zhao, J. -J. Xu and H. -Y. Chen, *Talanta*, 2009, **79**, 243.
  - 11 V. H. -C. Liao and K. -L. Ou, *Environ. Technol. Chem.*, 2005, **24**, 1624; J. Stocker, D. Balluch, M. Gsell, H. Harms, J. Feliciano, S. Daunert and J. R. Van Der Meer, *Environ. Sci. Technol.*, 2003, **37**, 4743.
  - 12 C. Liu, V. Balsamo, D. Sun, M. Naja, X. Wang, B. Rosen and C. -Z. Li, *Biosens. Bioelectron.*, 2012, **38**, 19; E. S. Forzani, K. Foley, P. Westerhoff and N. Tao, *Sens. Act. B*, 2007, **123**, 82.
  - 13 J. -H. Kwak, C. Lenth, C. Salb, E. -J. Ko, K. -W. Kim and K. Park, *Spectrochim. Acta Part B*, 2009, **64**, 1105.
  - 14 J. R. Kalluri, T. Arbneshi, S. A. Khan, A. Neely, P. Candice, B. Varsli, M. Washington, S. McAfee, B. Robinson, S. Banerjee, A. K. Singh, D. Senapati and P. C. Ray, *Angew. Chem.*, 2009, **121**, 9848.
  - 15 E. de Juan-Franco, A. Caruz, J. R. Pedrajas and L. M. Lechuga, *Analyst*, 2013, **138**, 2023; P. K. Jain, X. Huang, I. H. El-Sayed and M. A. El-Sayed, *Plasmonics*, 2007, **2**, 107; T. J. Park, S. J. Lee, D. -K. Kim, N. S. Heo, J. Y. Park and S. Y. Lee, *Talanta*, 2012, **89**, 246.
  - 16 N. A. Chaniotakis, K. Jurkschat, G. Reeske and A. Volosirakis, *Angew. Chem.*, 2001, **40**, 486.
  - 17 T. Kang, S. Oh, S. Hong, J. Moon and J. Yi, *Chem. Commun.*, 2006, 2998; J. N. Anker, W. P. Hall, O. Lyanders, N. C. Shah, J. Zhao and R. P. Van Duyne, *Nature Mater.*, 2008, **7**, 442; Y. -S. Chen, W. Frey, S. Kim, P. Kruizinga, K. Homan and S. Emelianov, *Nano Lett.*, 2011, **11**, 348; J. Jung, K. Na, J. Lee, K. -W. Kim and J. Hyun, *Anal. Chim. Acta*, 2009, **651**, 91; S. Oh, J. Moon, T. Kang, S. Hong and J. Yi, *Sens. Act. B*, 2006, **114**, 1096.
  - 18 V. Polshettiwar, D. Cha, X. Zhang and J. M. Basset, *Angew. Chem. Int. Ed.*, 2010, **49**, 9652.
  - 19 L. Saikia, D. Srinvas and P. Ratnasamy, *Micropor. Mesopor. Mater.*, 2007, **104**, 225.
  - 20 S. Hong, S. Lee and J. Yi, *Nanoscale Res. Lett.*, 2011, **6**, 336.
  - 21 S. Hong, S. Park, J. Park and J. Yi, *Coll. Surf. B*, 2013, **112**, 415.
  - 22 J. Janczak and G. J. Perpétuo, *Acta Cryst.*, 2008, **C64**, o330; S. Hong, S. Park, S. Lee, Y. I. Yang, H. D. Song and J. Yi, *Anal. Chim. Acta*, 2011, **694**, 136.
  - 23 U. Wirringa, H. W. Roseky, M. Noltemeyer and H. -G. Schmidt, *Angew. Chem.*, 1993, **32**, 1628.
  - 24 K. S. W. Sing, D. H. Everett, R. A. W. Haul, L. Moscou, R. A. Pierotti, J. Rouquérol and T. Siemieniowska, *Pure Appl. Chem.*, 1985, **57**, 603.